Failure analysis for railroad embankment under heavy haul wagon loads

Jin Shi*, Defeng Hou**

*Beijing Jiaotong University, Beijing 100044, China, E-mail: jshi@bjtu.edu.cn
**Beijing Jiaotong University, Beijing 100044, China

1. Introduction

With growing trends of railroads toward heavier axle loads, higher train speeds, and increasing amount of traffic, higher wheel loads will be exerted on the embankment with more repetition. Excessive embankment foundation deformation, which is often a major problem for railway, will produce high maintenance costs and reduced ride quality. According to the literature [1], foundation failure on the Coal Line were observed during 1994~1995 on the Vryheid-Richard Bay section, approximately 20 years after its initial construction.

Embankment foundation failure caused by large repetitive stresses in the embankment is progressive shear failure and excessive plastic deformation [2]. The design approach for preventing embankment failure is to limit the cumulative plastic strain. Various models have been developed for predicting cumulative plastic strain in soil under repeated loading. In general, the relationship between cumulative plastic strain and number of repeated stress is expressed exponential form [3]-[5]. Li et al [6] improve predicted method considers multilevel of deviator stresses and multisoil physical states that result from load-level variations, as well as seasonal and weather changes. Comparisons between predicted and experimental results show good applicability of the improved method. However, the method uses a value of deviator stress calculated by wheel load without considering vehicle/rail dynamic interaction.

Recent advances in remote condition monitoring techniques have facilitated the field measurement of railway track performance. This, together with the continuing increases in computer power which has enabled theoretical computational models of the track system to be developed, has furthered understanding of embankment failure in a dynamic loading environment.

Yang et al [7] investigated the train induced stress regime of the track substructure by means of a two-dimensional dynamic finite-element model (FEM). The model was used to analyse the effects of train speed, acceleration and braking, geometric variation in the rail head level, and hanging sleepers on the calculated stress. However, transient stress of embankment which was analysed is

unable properly to consider foundation failure due to repeated train passage.

In recent years, measurements and simulation of embankment culumulative plastic deformation induced by moving trains have been carried out by many railway research departments. Gräbe et al [8] measured permanent deformation of the track foundation, constructed in 2004 ,on the South African Coal Line, gathered over a period of 5 years. Permanent deformation measurements are used to calculate the design life of a foundation. However, little attention has been paid to the effect of rail irregularities, train speed and axle load on foundation failure in operation condition of heavy haul train.

In this paper, a dynamic three-dimensional finite element model using linear elastic material properties while including wheel-rail friction was developed and used to investigate embankment deviator stress. A method is developed for determining failure of embankment. The effect of train speeds, axle load, and rail irregularities on failure of embankment was investigated during repeated train passage. This is described further below.

2. Embankment foundation failures caused by wagon passage

Embankment foundation progressive shear failure and excessive plastic deformation (ballast pocket) under truck passage occur mainly in embankment comprised of fine-grained soils and can be related to embankment foundation cumulative plastic strain as represented by following equation [6]:

$$\varepsilon_p \left(\% \right) = a \left(\frac{\sigma_d}{\sigma_s} \right)^m N^b , \tag{1}$$

where ε_p is cumulative soil plastic strain, N is the number of repeated stress applications, σ_d is soil deviator stress caused by train dynamic load, σ_s is soil compressive strength, a, m, b are parameters dependent on soil type.

In three-dimensional stress state, σ_d can be determined using the following equation:

$$\sigma_d = \frac{\sqrt{\left[\left(\sigma_x' - \sigma_y' \right)^2 + \left(\sigma_y' - \sigma_z' \right)^2 + \left(\sigma_z' - \sigma_x' \right)^2 + 6 \left(\tau_{xy}^2 + \tau_{yz}^2 + \tau_{zx}^2 \right) \right]^2}}{2} , \tag{2}$$

where σ_x', σ_y' and σ_z' are the normal compressive effective stresses in the *x*, *y* and *z* directions respectively, and τ_{xy}, τ_{yz} and τ_{zx} are the shear stresses in the *xy*, *yz* and *zx* planes respectively.

For this study, the embankment foundation con-

sists of three distinct layers, the upper layer of stiff sand gravel(called "GL" for short.), and the middle layer consists of engineering filler made up of at least 50% gravel, sand and silt(called "FL" for short). The bottom layer is of medium strength sand silt (called "SL" for short). The material parameters of gravel and engineering filler were estimated from testing results of cyclic loads measured on Kongshan test section of Beijing-Shanghai railway in China [9].The values so determined in this study are given in Table 1.

In Table 1, σ_s is soil compressive strengths. For stiff, medium, and soft embankment, the range of soil compressive strength is about $200 \sim 350$ MPa, $100 \sim 200$ MPa and $35 \sim 100$ MPa respectively suggested by Li [6]. For this study, compressive strength of gravel and engineering filler which are stiff foundation were used value of upper limit and lower limit for stiff embankment respectively. Compressive strength of silt sand which is medium foundation was used lower value for medium embamkment. The soil compressive strengths for various soil types in this paper are shown in Table 1.

Table 1

Values of soil parameters for various soil type

Soil type	a	b	m	σ_s, MPa
Gravel	0.52	0.15	1.49	350
Filler	0.85	0.14	1.16	200
Silt sand	0.64	0.10	1.7	100

The number of load repetitions, N to which the embankment material would be subject was determined using Eq. (3):

$$N = \frac{T_d g}{8 L_s}, \tag{3}$$

where T_d is the total number of gross tones carried over the subgrade over the design life, L_s is static load.

The design approach for preventing foundation progressive shear failure is to limit the total cumulative plastic strain at the embankment foundation surface to below an allowable level for the period. This criterion is thus expressed by following equation:

$$\varepsilon_p \leq \varepsilon_{pa}, \tag{4}$$

where ε_{pa} is allowable plastic strain at the foundation surface for design period. Limiting value of plastic strain of $\varepsilon_{pa} = 2\%$ suggested by Li and Selig [2].

3. Development of a three-dimensional finite element model

In order to facilitate the design of appropriate embankment which would minimize vibration of the track components and track deterioration, a three dimensional dynamic finite element model (FEM) of the track vehicle system was built using ABAQUS explicit software.

The track components consisted of 75 kg/m continuously welded rail laid to a gauge of 1435 mm, supported by concrete sleepers placed at a spacing of 0.6 m. The ballast thickness is about 0.6 m. The embankment foundation consists of three distinct layers: the upper layer of stiff sand gravel (approximately 0.7 m deep), and the middle layer of 2.3 m deep consists of engineering filler made up of at least 50% gravel, sand and silt and is specified in the Chinese design standard to be of "Class A". The bottom layer of 3.0 m is of medium strength sand silt.

The embankment was modeled as a three-dimensional dynamic system. Solid linear elastic elements, with eight nodes, were used to model the rail, sleepers, ballast and embankment foundation. The embankment foundation was modeled as three layers. Parametric properties are given Table 2. In addition, vertical stiffness and damping of fastener are 78 kN/mm and 50 kN s/m. The length of embankment model in longitudinal was 100 m, the depth of model was set at 20 m. Infinite elements were used at the boundaries of the embankment to overcome the problem of the stress waves generated from being reflected back into the model. The finite element mesh, shown in Fig. 1, comprised of a total of 124357 elements and 176268 nodes.

Table 2

Materials properties parameters in FE model

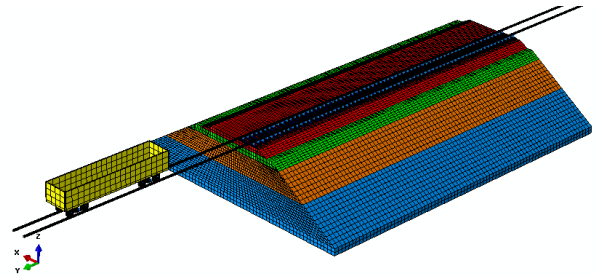| Component description	Young's modulus, MPa	Poisson's ratio	Density, kg/m³
Rail	210000	0.3	7830
Sleeper	35000	0.22	2600
Ballast	180	0.27	1650
Sand gravel	180	0.3	2300
Engineering filler A	130	0.3	2100
Silt sand	50	0.25	1800

Fig. 1 FE model for dynamic analysis

The wagon consists of a car body, bogie and wheel set, with spring-dashpot suspensions between those components as shown in Fig. 2. The associated parameters of those components are given in Table 3. The connections of suspension system are modelled as a system of linear springs and viscous dashpots in the vertical direction. Wagon vibration in the vertical plane only was considered. With the above assumptions, the car body is designated by vertical, pitching and rolling movements. For the bogie, vertical, pitching and rolling movements are considered. For the wheel set, vertical and rolling movements are considered. So the idealized model for a wagon can be described as 17 degrees of freedom.
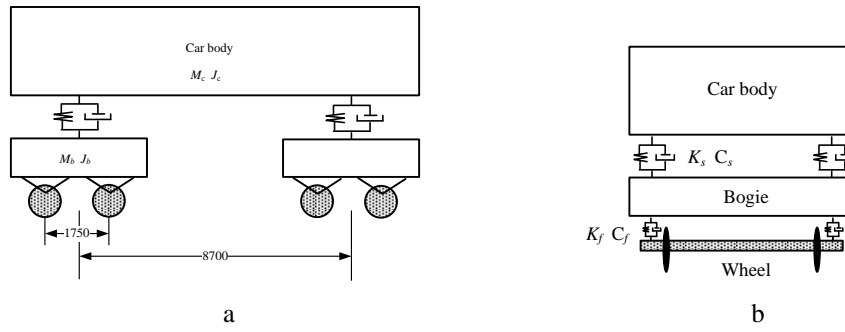
Fig. 2 Idealized freight vehicle: a - the vertical section; b - the cross section

Table 3

Wagon parameters

Mass of car body, M_c	91400 kg
Inertia of car body, J_c	1.33×10^5 kg m^2
Mass of bogie, M_b	1786 kg
Inertia of bogies, J_b	420 kg m^2
Mass of wheel, M_w	1257 kg
Primary suspension stiffness, K_f	13 MN/m
Primary suspension damping, C_f	3×10^5 Ns/m
Secondary suspension stiffness, K_s	4.4 MN/m
Secondary suspension damping, C_s	4×10^3 Ns/m

The contact normal force between the wheel and rail was modelled as Hertzian [10]. The normal contact force $P(t)$ can be determined using the following equation:

$$P(t) = \left(\frac{1}{G} \Delta Z(t) \right)^{3/2}, \tag{5}$$

where $\Delta Z(t)$ is the elastic compression between the rail and wheel (in m), G is the contact constant and is given by:

$$G = 3.86 \, R^{-0.115} \times 10^{-8} \text{ (m/N}^{3/2}), \tag{6}$$

where R is radius of wheel.

The creep force between the wheel-rail is given by:

$$\tau_{crit} = \mu p, \tag{7}$$

where μ is the coefficient of friction which was set to 0.3.

4. Failure analysis for embankment foundation

4.1. Effect of train speed

In this section, the effect of train speed on foundation stress, cumulative strain and design life were investigated. In the FE model, the wagon with axle load of 250 kN ran along the rail at speeds of 40, 60, 80, 100, 120 km/h. The annual tonnage of 100, 200, 300 and 400 Mt were selected to estimate life of embankment.

Fig. 3, a shows the calculated deviator stress at different depth of foundation at different train speeds. Fig. 3, b shows the calculated cumulative plastic strain at different depth of foundation at different train speeds. According to the strain criteria (2%), the number of cycles and the life for foundation failure is summarized in Fig. 3, c and Table 4 respectively.
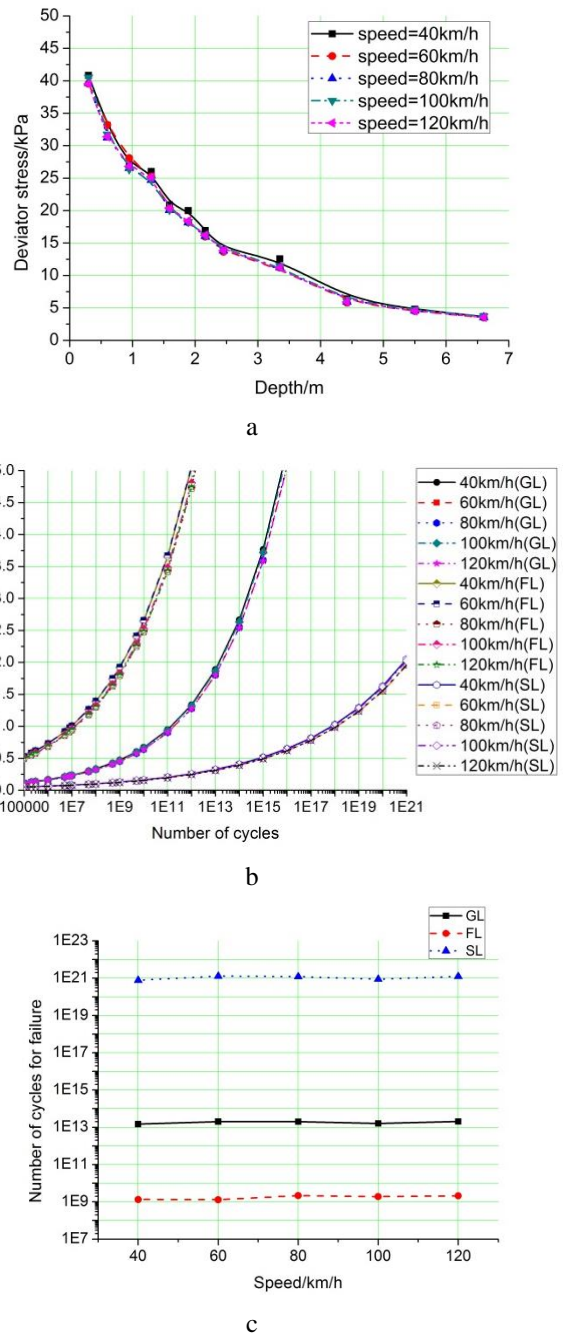

a

b

c

Fig. 3 The effect of train speed on foundation failure: a - deviator stress at different depth of foundation at different train speeds; b - cumulative plastic strain at different depth of foundation at different train speeds; c - the number of cycles for foundation failure

The analysis indicates that increasing train speed has little effect on foundation failure in current operation speed range (speed < 120 km/h). It can be seen that failure occurs first in filler layer instead of gravel layer, and there is a rapidly decrease in foundation life which was deter-mined by fill layer failure as annual tonnage is increased. As annual tonnage is increased beyond 400 Mt, the foundation life cannot meet a projected design life of 40 years. This means that rehabilitation should be commenced to meet mass transit.

Table 4

Life of foundation at different train speeds

Speed, km/h	Number of cycles for foundation failure	The total number of gross tones for foundation failure, Mt	Design life of foundation, year			
			100 Mt	200 Mt	300 Mt	400 Mt
40	1.33×10^9	13300	133	66.5	44.3	33.3
60	1.31×10^9	13100	131	65.5	43.7	32.8
80	2.17×10^9	21700	217	108.5	72.3	54.3
100	1.90×10^9	19000	190	95	63.3	47.5
120	2.10×10^9	21000	210	105	70	52.5

4.2. Effect of axle load

In this section, the effect of axle load on founda-tion stress, cumulative strain and design life were investi-gated. At heavy haul railway, a typical wagon may apply the axle load of 210 kN and 250 kN, the wagon with axle load of 300 kN will be applied to increase volume in the future. The speed of the wagon running through the sub-grade was 100 km/h.
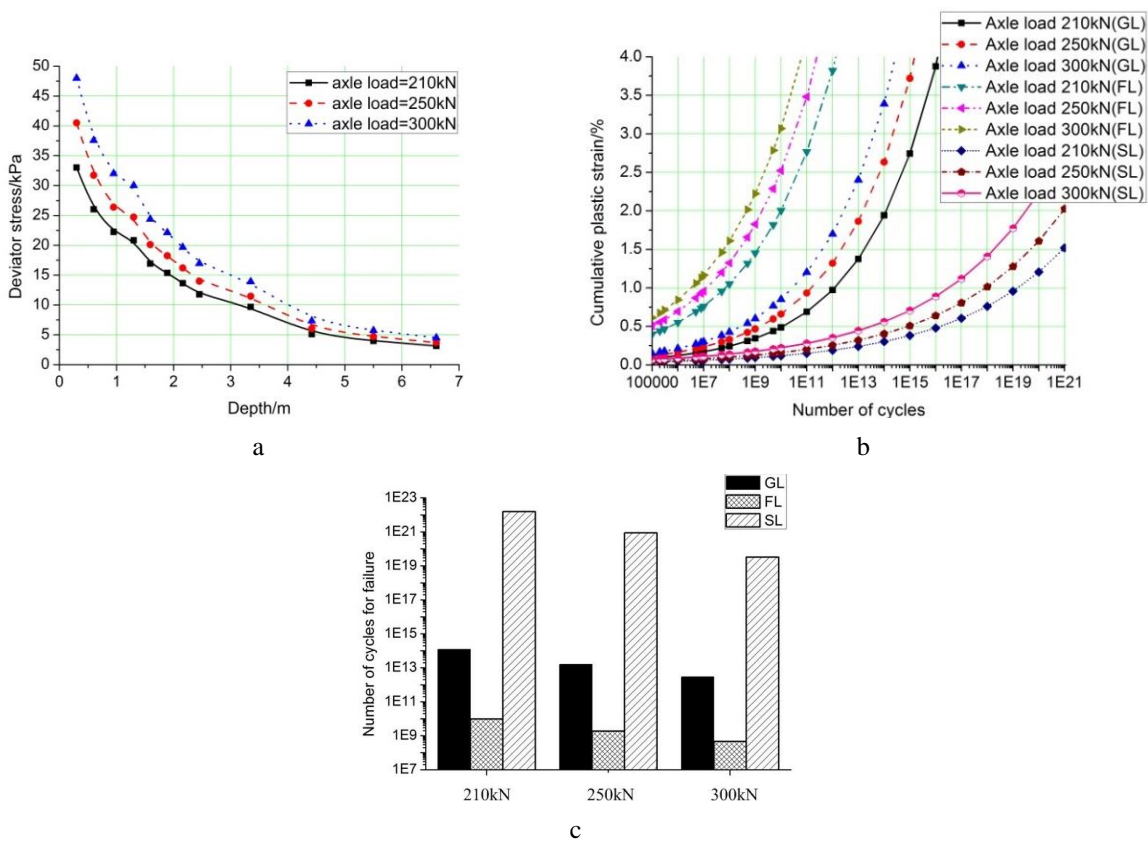
a

b

c

Fig. 4 The effect of axle load on foundation failure: a - deviator stress for three types of axle load at different depth of foundation; b - cumulative plastic strain for three types of axle load at different depth of foundation; c - the number of cycles for foundation failure

Fig. 4, a shows the calculated deviator stress for three types of axle load at different depth of foundation. The effect of the change in axle load on the deviator stress-es is such that the calculated deviator stress increase in the foundation caused by a wagon with an axle load of 300 kN is greater than for an axle load of 250 kN for a wagon moving, and the deviator stress caused by a wagon with axle load of 250 kN is greater than for an axle load of 210 kN. This is particularly evident at depth of 0 ~ 4 m in foundation.

Fig. 4, b shows the calculated cumulative plastic strain for three types of axle load at different depth of foundation. As with the cumulative plastic strain of foun-dation, there is a gradual increase in plastic strain as the

axle load increase from 210 to 300 kN. According to the strain criteria, the number of cycles and the life for foundation failure is summarized in Fig. 4, c and Table 5 respectively. It can be seen that failure occurs first in filler layer instead of gravel layer, and there is a rapidly decrease in foundation life which was determined by fill layer failure as axle load is increased. The life of foundation for axle load of 250 kN is about 80% less than for axle load of

210 kN, and the life for axle load of 300 kN is about 75% less than for axle load of 250 kN. The analysis also showed that the foundation life with axle load of 300 kN is less than 60 years for annual tonnage 100 Mt, 30 years for annual tonnage 200 Mt, 20 years for annual tonnage 300 Mt, 15 years for annual tonnage 400 Mt.This suggests that the foundation should be upgraded to handle wagon trains with axle load of 300 kN.

Table 5

Life of foundation with different types of axle load

Axle load, kN	Number of cycles for foundation failure	The total number of gross tones for foundation failure, Mt	Design life of foundation, year			
			100 Mt	200 Mt	300 Mt	400 Mt
210	9.80×10^9	82400	824	412	275	206
250	1.90×10^9	19000	190	95	63.3	47.5
300	4.69×10^8	5630	56.3	28.2	18.8	14.1

4.3. Effect of rail irregularities

Rail irregularities are a major source of vibration for moving trains. In railway engineering practice, the track irregularity is frequently characterized by the one-sided power spectral density (PSD) function of the track geometry. The PSD functions used in the study are given as follows [11]:

$$S_v\left(\Omega\right) = \frac{kA_v\Omega_c^2}{\Omega^2\left(\Omega^2 + \Omega_c^2\right)},$$ (8)

where $S_v\left(\Omega\right)$ is a power spectral density(PSD) function ,cm^2/(rad/m); A_v is the irregularities coefficient, cm^2 rad/m; $\Omega = 1/\lambda$ denotes the spatial frequency, Hz; λ is the length of the irregularity, m; Ω_c is frequencies than change the shape of $S_v\left(\Omega\right)$, k is safety coefficient (0.25).

Table 6 contains the values for the coefficients involved in Eq. (8), which are equivalent to classes 5 and 6 of track classification used by the Federal Railroad Administration (FRA). The track classes refer to track designations that range from 1 to 6, with class 6 indicating the best and class 1 the worst. In the study, class 6 and 5 were selected to simulate good and poor quality rail.

Table 6

The values for the coefficients of PSD functions

Quality	Ω_c, rad/m	A_v, cm^2 rad/m	Maximum speed, km/h
Poor(FRA5)	0.8245	0.2095	128
Good(FRA6)	0.8245	0.0339	176

By applying the spectral representation method, rail irregularities time domain samples for FRA5 and FRA6 were shown in Fig. 5. Fig. 5 shows the maximum amplitude of moderate and poor quality rail are 5 mm and 10 mm respectively.

In this section, the effect of irregularities on foundation stress, cumulative strain and design life were investigated. In FE model, the wagon with axle load 250 kN ran
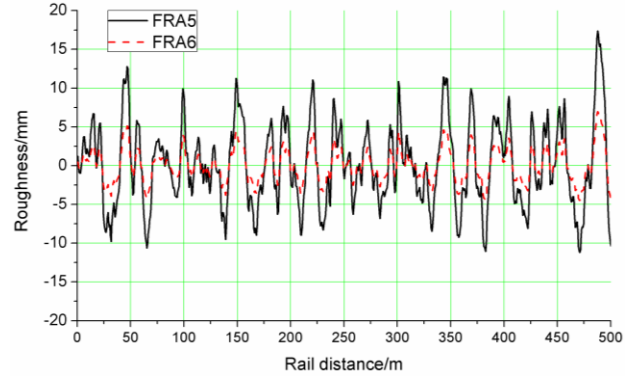
at a speed of 100 km/h.

Fig. 5 Rail irregularities in time domain

Fig. 6, a shows the calculated deviator stress for three types of rail irregularities at different depth of foundation. Values of deviator stress with FRA6 or without irregularities are very different, but the values with FRA5 are greater than those of the other two cases. From these it is evident that train-induced vibrations under poor irregularities have important influence on the stress of foundation and suggests that the irregularities for amplitude of more than 5 mm will accelerate deterioration in the foundation.

Fig. 6, b shows the calculated cumulative plastic strain for three types of rail irregularities at different depth of foundation. It may be seen that the cumulative plastic strain with FRA5 irregularities are always higher than that with FRA6 or without irregularities. According to the strain criteria, the number of cycles and the life for foundation failure is summarized in Fig. 6, c and Table 7 respectively. It can be seen that failure occurs first in filler layer instead of gravel layer. Poor quality irregularities reduce the life of the foundation by approximately 75 ~ 80%.The analysis also showed that the foundation life with FRA5 irregularities are less than 40 years for annual tonnage 100 Mt, 20 years for annual tonnage 200 Mt, 15 years for annual tonnage 300 Mt, 10 years for annual tonnage 400 Mt. This suggests that the rail maintainment should be strengthen to prevent foundation shear failure in short time.
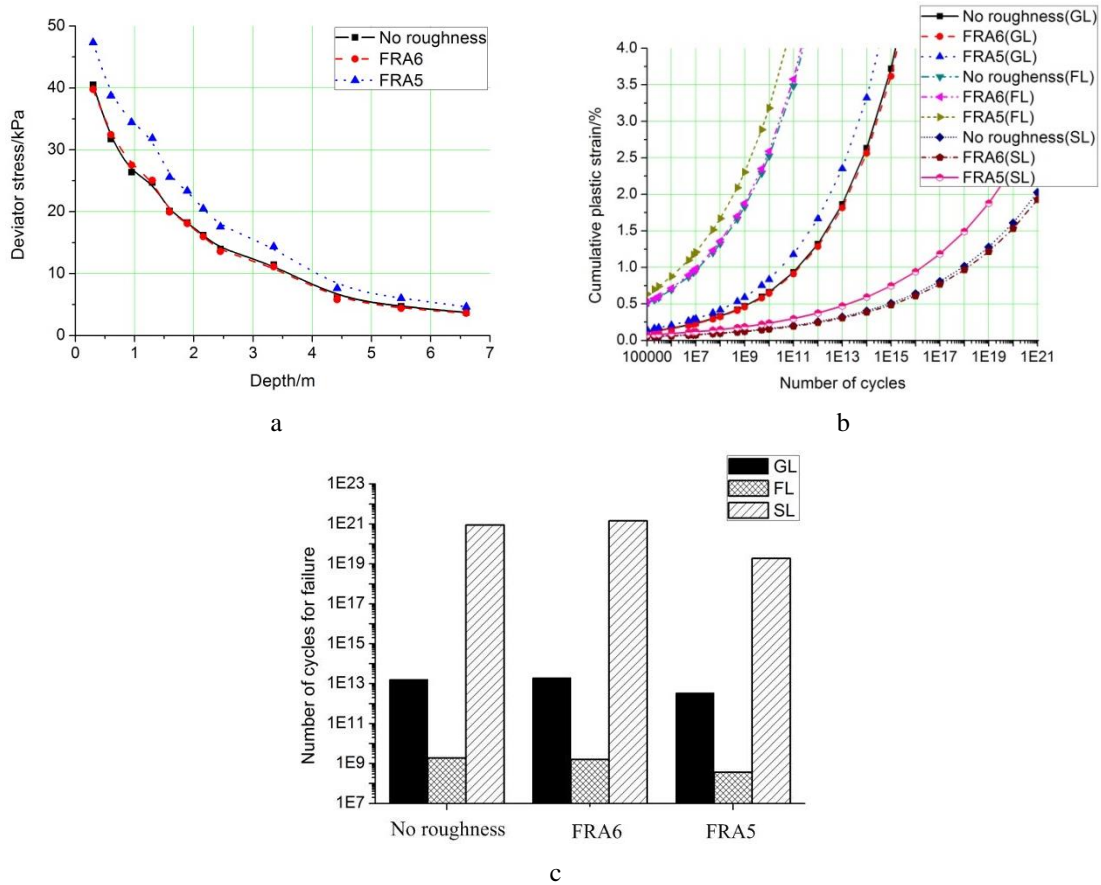
a

b

c

Fig. 6 The effect of irregularities on foundation failure: a - deviator stress for three types of rail irregularities at different depth of foundation; b - cumulative plastic strain for three types of rail irregularities at different depth of foundation; c - the number of cycles for foundation failure

Table 7

Life of foundation with different types of irregularities

Track condition	Number of cycles for foundation failure	The total number of gross tones for foundation failure, Mt	Design life of foundation (year)			
			100 Mt	200 Mt	300 Mt	400 Mt
Without irregularities	1.90×10^9	19000	190	95	63.3	47.5
FRA6	1.58×10^9	15800	158	79	52.7	39.5
FRA5	3.64×10^8	3640	36.4	18.2	12.1	9.1

5. Conclusions

A dynamic three-dimensional finite element model using linear elastic material properties while including wheel-rail friction was developed and used to investigate embankment deviator stress.

A method is developed for determining failure of embankment. The effect of train speeds, axle load, and rail irregularities on failure of embankment was investigated during repeated train passage.

Train speed has little effect on foundation failure in current operation speed range (speed < 120 km/h), however, axle load and irregularities have important effect on foundation failure. This suggests that the foundation should be upgraded to handle wagon trains with axle load of 300 kN, and rail maintainment should be strengthen to prevent foundation shear failure in short time .

Embankment failure occurs first in filler layer instead of gravel layer, and there is a rapidly decrease in foundation life which was determined by fill layer failure as annual tonnage is increased. As annual tonnage is increased beyond 400 Mt, the foundation life cannot meet a projected design life of 40 years. This means that rehabilitation should be commenced to meet mass transit.

6. Acknowledgements

References

1. **Gräbe, P.J.; Shaw, F.J.** 2009. Design life prediction of a heavy haul track foundation, Proc. IMechE, Part F: J. Rail and Rapid Transit 224(1): 337-344.
2. **Li, D.;Selig, E.T.** 1998. Method for railroad track foundation design. I: Development, Journal of Geotechnical and Geoenvironmental Engineering, ASCE 124(4):316-322.
http://dx.doi.org/10.1061/(ASCE)1090-

0241(1998)124:4(316).

3. **Monismith, C.L.; Ogawa, N.; Freeme, C.R.** 1975. Permanent deformation characteristics of subgrade soils due to repeated loading, Transportation Research Board 537: 1-17.

4. **Burrow, M.P.N.; Chan, A.H.C.** 2007. Deflectometer-based analysis of ballasted railway tracks, Geotechnical Engineering 160(GE3): 169-177.
   http://dx.doi.org/10.1680/geng.2007.160.3.169.

5. **Ju, S.H.; Liao, J.A; Ye, Y.L.** 2009. Behavior of ground vibration induced by trains moving on embankments with rail roughness, Soil Dynamics and Earthquake Engineering 20: 1237-1249.

6. **Li, D.; Selig, E.T.** 1994. Resilient modulus for fine-grained subgrade soils, Journal of Geotechnical Engineering, ASCE 120(6): 939-957.
   http://dx.doi.org/10.1061/(ASCE)0733-9410(1994)120:6(939).

7. **Yang, L.A.; Powrie, W.; Priest, J.A.** 2009. Dynamic stress analysis of a ballasted railway track bed during train passage, Journal of Geotechnical and Geoenvironmental Engineering 135(5): 680-689.
   http://dx.doi.org/10.1061/(ASCE)GT.1943-5606.0000032.

8. **Gräbe, P.J.; Clayton, C.R.I.** 2009. Effects of principal stress rotation on permanent deformation in rail track foundations, Journal of Geotechnical and Geoenvironmental Engineering 135(4): 555-565.
   http://dx.doi.org/10.1061/(ASCE)1090-0241(2009)135:4(555).

9. **Dong, L.; Cai, D.G.; Zhao, C.G.** 2010. Method for predicting the cumulative deformation of high-speed railway subgrade under cyclic train loads, China Civil Engineering Journal 43(6): 100-108. (in Chinese)

10. **Zhai, W.M.; Wang, K.Y.; Lin, J.H.** 2007. Modeling and experiment of railway ballast vibrations, Journal Sound and Vibration 270(4): 673-683.

11. **Fries, R.H.; Coffey, B.M.** 1990. A state-space approach to the synthesis of random vertical and cross-level rail irregularities, Journal Dynamic System, Measurement and Control 112(1): 83-87.
    http://dx.doi.org/10.1115/1.2894143.

Jin Shi, Defeng Hou

FAILURE ANALSIS FOR RAILROAD EMBANKMENT UNDER HEAVY HAUL WAGON LOADS

S u m m a r y

In this paper, a dynamic three-dimensional finite element model using linear elastic material properties while including wheel-rail friction was developed and used to investigate embankment deviator stress. The effect of train speeds, axle load, and rail roughness on failure of embankment was investigated during repeated train passage. Results indicate that axle load and rail roughness have important effect on foundation failure. Embankment failure occurs first in engineering filler layer instead of gravel layer, and there is a rapidly decrease in foundation life which was determined by fill layer failure as annual tonnage is increased. As annual tonnage is increased beyond 400 Mt, the foundation life cannot meet a projected design life of 40 years.